Published in final edited form as:
Opt Lett. 2011 April 1; 36(7): 1029–1031.

In vivo integrated photoacoustic and confocal microscopy of hemoglobin oxygen saturation and oxygen partial pressure

Yu Wang, **Song Hu**, **Konstantin Maslov**, **Yu Zhang**, **Younan Xia**, and **Lihong V. Wang**[*]
Department of Biomedical Engineering, Washington University in St. Louis, Campus Box 1097, One Brookings Drive, St. Louis, MO 63130-4899, USA

Abstract

A dual-modality microscope integrating photoacoustic microscopy and fluorescence confocal microscopy was developed to noninvasively image hemoglobin oxygen saturation (sO_2) and oxygen partial pressure (pO_2) *in vivo* in single blood vessels with high spatial resolution. While photoacoustic microscopy measures sO_2 by imaging hemoglobin optical absorption at two wavelengths, fluorescence confocal microscopy quantifies pO_2 using phosphorescence quenching. The variations of sO_2 and pO_2 values in multiple orders of vessel branches under hyperoxic (100% oxygen) and normoxic (21% oxygen) conditions correlate well with the oxygen-hemoglobin dissociation curve. In addition, the total concentration of hemoglobin is imaged by photoacoustic microscopy at an isosbestic wavelength.

Understanding of oxygen transport and consumption *in vivo* is of great significance to studies of angiogenesis and tumor growth. The oxygen partial pressure, pO_2, is proportional to dissolved oxygen concentration, and directly measures the oxygen available to cells. The percentage of hemoglobin saturated with oxygen, sO_2, quantifies the amount of oxygen carried by blood hemoglobin. Both pO_2 and sO_2 are important hemodynamic parameters for oxygen metabolism. Moreover, the relationship of pO_2 and sO_2 describes the binding affinity of hemoglobin for oxygen. The *in vivo* measurement of the oxygen-hemoglobin dissociation curve describes how our blood carries and releases oxygen under physiological and pathological conditions.

Photoacoustic microscopy (PAM), which can spectroscopically measure hemoglobin absorption [1], is ideal for high resolution imaging of sO_2 *in vivo*. Other imaging modalities, such as optical coherence tomography and reflectance absorbance spectroscopy, have been used to map sO_2 [2,3]. However, tissue scattering and the nonlinear relationship between signal intensity and absorption coefficients made their sO_2 quantifications problematic. Besides, two-dimensional reflectance absorbance spectroscopy also suffers from blood volume fluctuation. PAM, on the other hand, is 100% sensitive to optical absorption, fairly insensitive to scattering, and capable of volumetric imaging [4]. The use of phosphorescence lifetime quenching for measuring pO_2 in vasculature has been well established [5–7]. In our studies, a generally used phosphorescent probe, Pd-meso-tetra (4-carboxyphenyl) porphyrin (PdT790, Frontier Scientific), was chosen for its peak absorption wavelength of 524 nm. The oxygen sensitive phosphorescent probe was injected into the systemic vasculature and excited by light. The resulting phosphorescent emission was quenched by intravascular oxygen. As described by the Stern-Volmer equation, the phosphorescence decay time can be

[*]Corresponding author: lhwang@biomed.wustl.edu.

OCIS Codes: 170.3880, 170.5120, 170.1790, 180.5810

converted to the intravascular pO_2. Here, we present a dual-modality microscope combining photoacoustic microscopy and fluorescence confocal microscopy (FCM), designed for imaging both blood sO_2 and pO_2 *in vivo*. By modulating the inspiratory oxygen concentration, the sO_2 and pO_2 responses can be correlated to study oxygen hemoglobin binding.

A schematic of the integrated photoacoustic and fluorescence confocal microscopy (PA-FCM) system is presented in Fig. 1. Details about the PA-FCM system design and performance have been published previously [8]. The system employs a dye laser (CBR-D, Sirah) with tunable wavelengths in the range of 560–590 nm (Rhodamine 6G, Exciton), pumped by a 523 nm Nd:YLF laser (INNOS-LAB, Edgewave). The 523 nm pump laser pulses excite the oxygen-sensitive phosphorescent probe; the wavelength-tunable dye laser pulses are used to image hemoglobin absorption at multiple wavelengths. The generated phosphorescent light and photoacoustic wave are collected by a photomultiplier tube module (H9307-03, Hamamatsu, Bandwidth, DC–200 kHz) and a 75-MHz ultrasonic transducer (V2022 BC, Olympus NDT), respectively. The phosphorescent light passes through a dichroic mirror (DMLP605, Thorlabs) and a emission filter (FEL0650, Thorlabs). A 150 μm diameter emission pinhole suppresses the out-of-focus phosphorescent light rays. To compensate the photoacoustic amplitude for laser fluence fluctuation, the laser pulses are sampled by a photodiode (SM05PD1A, Thorlabs). The amplified photoacoustic or phosphorescence signals are acquired and saved along with the laser fluence signals by a DAQ instrument (CS 14200, Gage Applied).

Nude mouse (Harlan, body weight ~20 g) ears were imaged to demonstrate the dual-modality microscopy of sO_2 and pO_2 *in vivo*. All experimental animal procedures were carried out in conformity with the laboratory animal protocol approved by the Animal Studies Committee of Washington University in St. Louis.

The PdT790 (10 mg/ml) was conjugated with bovine serum albumin (60 mg/ml) in 0.9% NaCl solution to provide a uniform environment for bound phosphors [5]. A 0.1 ml volume of the phosphorescent probe solution was bolus injected into the systemic vasculature via the tail vein. To allow the probe to equilibrate in the blood, image acquisition started 10 min after injection.

Photoacoustic images at wavelengths of 570 nm and 578 nm were captured. From the photoacoustic amplitude, aided by the molar absorption spectra of oxygenated hemoglobin (HbO_2) and deoxygenated hemoglobin (HbR), the relative concentrations of HbO_2 and HbR, and subsequently sO_2, were calculated [1]. To measure the phosphorescence quenching, the phosphorescent light intensity was acquired for 500 μs at a sampling rate of 20 MHz. The relationship of pO_2 and the phosphorescence lifetime was assumed to follow the Stern-Volmer equation:

$$\tau^{-1}=\tau_0{}^{-1}+k_q \cdot pO_2 \quad (1)$$

where τ_0 is the lifetime in the absence of O_2 and k_q is the quenching constant. The constants τ_0 and k_q have been experimentally calibrated and published in the literature [5,9]. We used the quenching constants for pH = 7.4 and temperature = 23 °C (τ_0 = 711 μs, k_q = 259 $mmHg^{-1}s^{-1}$) [3]. A detailed description of the method used for computing sO_2 and pO_2 can be found in review articles [1,5].

To study the relationship of pO_2 and sO_2 *in vivo*, the blood pO_2 and sO_2 levels were modulated by switching the physiological state from systemic hyperoxia to normoxia in a

mouse. Hyperoxia was induced by changing the inhalation gas to 100% O_2, and the mouse was returned to normoxia by changing the inhalation gas to air. Prior to imaging, the mouse was exposed to each oxygen concentration for 10 min to stabilize the hyperoxic and normoxic states.

First, to explore the mapping of pO_2 and sO_2, we imaged a nude mouse ear under hyperoxia. Figure 2(a) shows a photoacoustic image of the mouse ear vasculature acquired at 570 nm, an isosbestic wavelength where HbO_2 and HbR have identical molar absorption coefficients. Thus the photoacoustic amplitude measures the total hemoglobin (HbT) concentration. By combination with another photoacoustic image acquired at 578 nm, a pixel by pixel map of sO_2 was computed. As shown in Fig. 2(b), the arterioles and venules are visualized in pseudocolors of red and green, based on the different sO_2 levels. Figure 2(c) shows the time-integrated phosphorescence image, where sebaceous glands and blood vasculature can be seen as speckle and tree features, respectively. Autofluorescence from tissue often has a sub-microsecond lifetime, while the phosphorescence from the palladium porphyrin phosphorescent probe features ~100 μs decay time. We split the phosphorescence signal at 5 μs so that the images of sebaceous glands (Fig. 2(d)) and blood vasculature (Fig. 2(e)) are separated. Figure 2(f) plots example phosphorescence decay curves measured in the artery and vein labeled with arrows in Fig. 2(e). The phosphorescence lifetime was determined by fitting the measured data to an exponential decay curve (R_2 = 0.98 for arterial data and 0.99 for venous data). The shorter lifetime for the arterial data (71 μs) compared with that for the venous data (156 μs) shows phosphorescence quenching by dissolved blood oxygen. Pixelwise fitting produces a map of phosphorescence lifetime (Fig. 2(g)), which is further converted through Eq. (1) to a map of pO_2 (Fig. 2(h)). A comparison of Figs. 2(b) and (h) shows that the blood vessels with higher sO_2 values measured by PAM have correspondingly higher pO_2 values measured by FCM, which agrees with known physiology [10].

To closely investigate the pO_2 and sO_2 levels in response to oxygen variation, sO_2 and pO_2 in hyperoxia (100% oxygen) and normoxia (21% oxygen) were mapped. We selectively analyzed an ~1.5×1.5 mm^2 area of a mouse ear that contained four microvascular branching orders, as shown in Fig. 3(a) (photoacoustic image) and Fig. 3(b) (phosphorescence image). Figures 3(c–f) show the sO_2 and pO_2 mappings for hyperoxic and normoxic conditions. Our results suggest that switching from hyperoxia to normoxia elicited a decrease in both sO_2 and pO_2 levels. They further suggest that in the artery, the sO_2 remained high (>80%) while the pO_2 dropped significantly (from >100 mmHg to ~30 mmHg). In the vein, the decrease of sO_2 (from ~80% to ~70%) was correlated with a smaller decrease in pO_2 (from ~35 mmHg to ~20 mmHg). Our observation is in agreement with the sigmoidal shape of the oxygen hemoglobin dissociation curve (OHDC). The precapillary arteriolar and postcapillary venular trees are drawn in red and blue, respectively, in Fig. 3(g). The vasculature in the imaged region is segmented by different branching orders, and the sO_2 and pO_2 values were averaged within each segment (the correlation coefficient between sO_2 and pO_2 values = 0.62). We compared the experimental data with the classic OHDC equation developed by Kelman [11],

$$sO_2 = 100 \times \frac{a_1 + a_2 x^2 + a_3 x^3 + x^4}{a_4 + a_5 x + a_6 x^2 + a_7 x^3 + x^4} \quad (2)$$

where a_{1-7} are coefficients calibrated at the standard condition (temperature T = 37 °C, pH = 7.4, and CO_2 partial pressure pCO_2 = 40 mmHg), and

$$x = f(T, pH, pCO_2) \times pO_2 \tag{3}$$

$$f = 10^{[-0.024(T-37)+0.40(pH-7.40)-0.06(\log_{10} pCO_2 - \log_{10} 40)]} \tag{4}$$

The conversion factor f alters the scale of the pO_2 axis in response to changes of temperature, pH and CO_2 partial pressure [11]. Although both the blood pH and pCO_2 vary with the vasculature order and the physiological state [12], the OHDC maintains the sigmoidal shape. To demonstrate the non-linear tendency for oxygen to bind to hemoglobin in the measured data, we applied a least-squares fitting of the pO_2 and sO_2 values to the above Kelman's equation with f being the fitting parameter. The fitted curve ($f = 1.83$) rises steeply with increasing pO_2 and reaches 90% sO_2 at pO_2 of 32 mmHg. The correlation coefficient between the fitted and measured sO_2 values was 0.67.

In summary, we developed an integrated PA-FCM system to image sO_2 and pO_2 as well as the total concentration of hemoglobin vessel by vessel *in vivo*. The ability to extract noninvasively sO_2 and pO_2 information in individual vessels makes the dual-modality microscope system a potential tool for quantitative analysis of oxygen transport and consumption in tissues.

Acknowledgments

We thank C. Zhang for helping with data processing and manuscript preparation. This work was sponsored in part by National Institutes of Health (NIH) grants R01 EB000712, R01 EB008085, R01 CA134539, U54 CA136398, and 5P60 DK02057933. L. Wang has a financial interest in Microphotoacoustics, Inc., and Endra, Inc., which, however, did not support this work.

References

1. Hu S, Wang LV. Photoacoustic imaging and characterization of the microvasculature. J. Biomed. Opt. 2010; 15:011101. [PubMed: 20210427]
2. Faber D, Mik E, Aalders M, van Leeuwen T. Toward assessment of blood oxygen saturation by spectroscopic optical coherence tomography. Opt. Lett. 2005; 30:1015–1017. [PubMed: 15906988]
3. Shonat RD, Wachman ES, Niu W, Koretsky AP, Farkas DL. Near-simultaneous hemoglobin saturation and oxygen tension maps in mouse brain using an AOTF microscope. Biophys. J. 1997; 73:1223–1231. [PubMed: 9284290]
4. Zhang C, Maslov K, Wang L. Subwavelength-resolution label-free photoacoustic microscopy of optical absorption in vivo. Opt. Lett. 2010; 35:3195–3197. [PubMed: 20890331]
5. Lo L-W, Koch CJ, Wilson DF. Calibration of oxygen-dependent quenching of the phosphorescence of Pd-meso-tetra (4-carboxyphenyl) porphine: a phosphor with general application for measuring oxygen concentration in biological systems. Anal. Biochem. 1996; 236:153–160. [PubMed: 8619481]
6. Yaseen M, Srinivasan V, Sakadzic S, Wu W, Ruvinskaya S, Vinogradov S, Boas D. Optical monitoring of oxygen tension in cortical microvessels with confocal microscopy. Opt. Express. 2009; 17:22341–22350. [PubMed: 20052157]
7. Estrada A, Ponticorvo A, Ford T, Dunn A. Microvascular oxygen quantification using two-photon microscopy. Opt. Lett. 2008; 33:1038–1040. [PubMed: 18483504]
8. Wang Y, Maslov K, Kim C, Hu S, Wang LV. Integrated photoacoustic and fluorescence confocal microscopy. IEEE Trans. Biomed. Eng. 2010; 57:2576–2578. [PubMed: 20639165]
9. Sinaasappel M, Ince C. Calibration of Pd-porphyrin phosphorescence for oxygen concentration measurements in vivo. J. Appl. Physiol. 1996; 81:2297–2303. [PubMed: 8941557]

10. Adair GS. The hemoglobin system: VI. the oxygen dissociation curve of hemoglobin. J. Biol. Chem. 1925; 63:529–545.
11. Kelman GR. Digital computer subroutine for the conversion of oxygen tension into saturation. J. Appl. Physiol. 1966; 21:1375–1376. [PubMed: 5916678]
12. Kobayashi H, Takizawa N. Oxygen saturation and pH changes in cremaster icrovessels of the rat. Am. J. Physiol. Heart Circ. Physiol. 1996; 270:1453–1461.

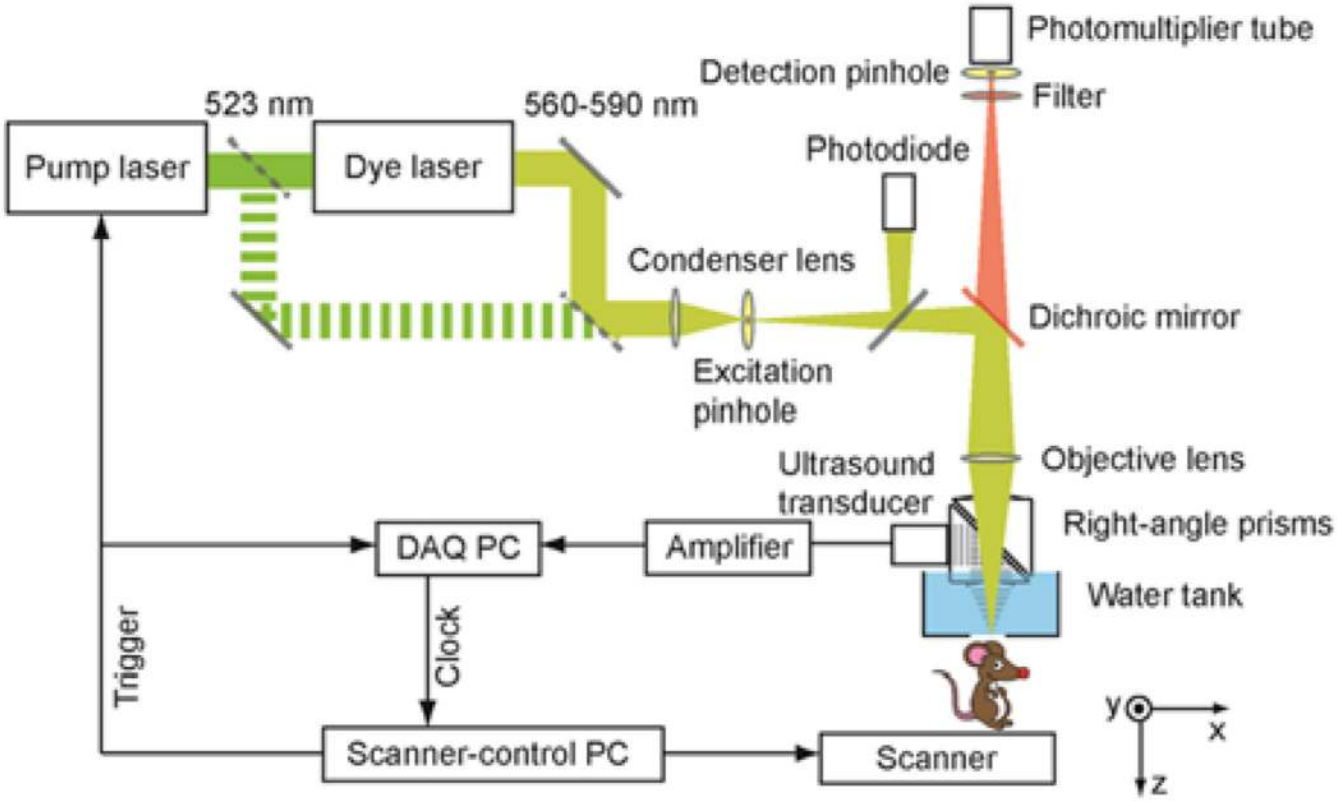

Fig. 1.
(Color online) Schematic of the integrated photoacoustic and confocal microscopy setup.

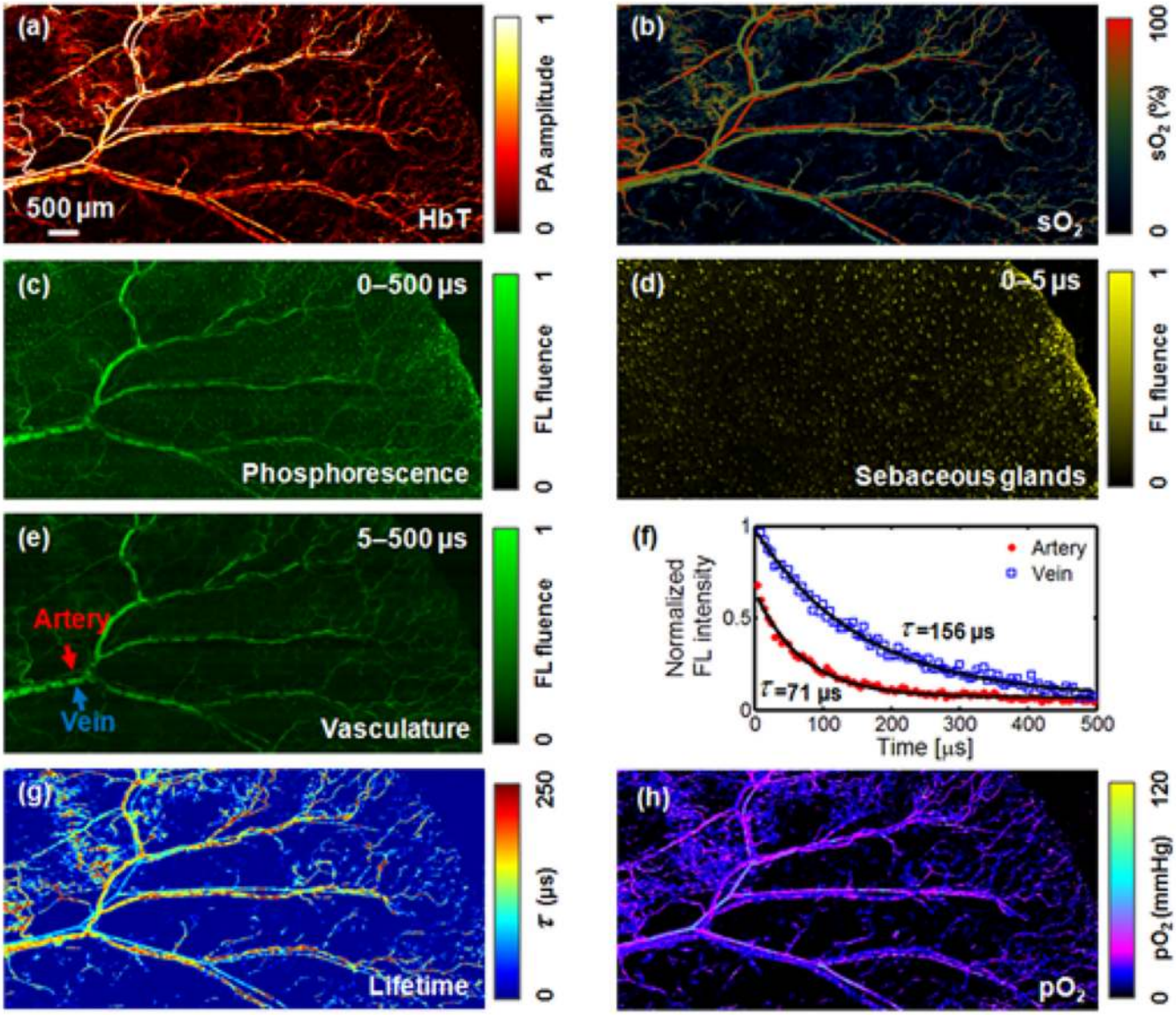

Fig. 2.

(Color online) Imaging of the ear of a mouse in hyperoxia *in vivo*. (a) Photoacoustic image of total concentration of hemoglobin acquired at isosbestic 570 nm. (b) Photoacoustic image of sO_2 acquired at 570 and 578 nm. (c) Confocal image of time-integrated phosphorescence excited at 523 nm. Sebaceous glands and blood vessels are separated in the confocal images by integrating the phosphorescence signal (d) before and (e) after 5 µs. (f) Phosphorescence decay curves from two regions of 15×15 pixels each in the artery and vein indicated by the arrows in (e). (g) Confocal image of the phosphorescence lifetime. (h) Confocal image of pO_2. PA: photoacoustic; FL: fluorescence. HbT: total hemoglobin concentration. τ: phosphorescence lifetime.

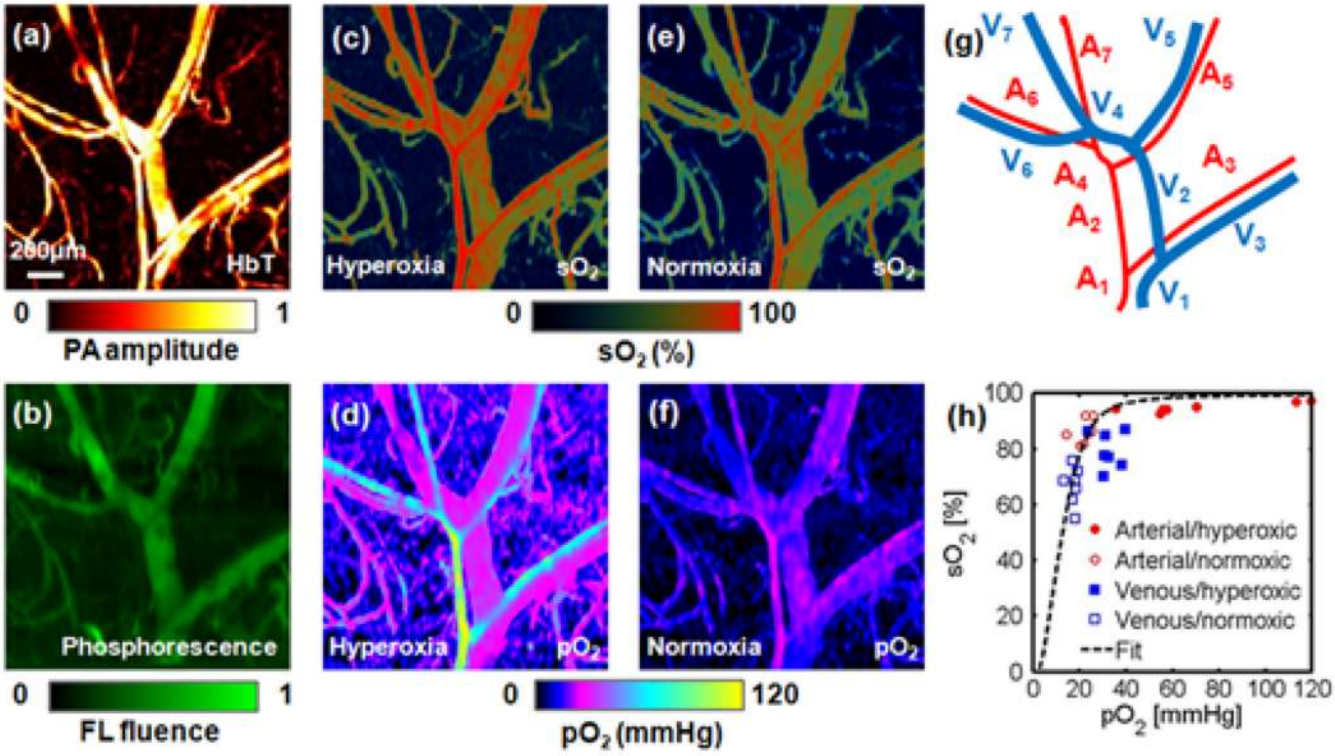

Fig. 3.

(Color online) Photoacoustic and confocal microscopy of pO_2 and sO_2 levels in the ear of a mouse in response to switching from hyperoxia to normoxia. (a) Photoacoustic image of total concentration of hemoglobin acquired at 570 nm. (b) Confocal image of time-integrated phosphorescence in the same region excited at 523 nm. (c) Photoacoustic image of sO_2 and (d) confocal image of pO_2 in hyperoxia. (e) Photoacoustic image of sO_2 and (f) confocal image of pO_2 in normoxia. (g) Skeletons of arteries (Ai) and veins (Vi) shown in (a), where subscript i denotes the segmentation. (h) Plot of sO_2 versus pO_2 values in arteries and veins identified in (g). PA: photoacoustic; FL: fluorescence. HbT: total hemoglobin concentration.